

Universally Robust Graph Neural Networks by Preserving Neighbor Similarity

Yulin Zhu

yulinzhu@polyu.edu.hk

The Hong Kong Polytechnic University
HKSAR, China

Xing Ai

xing96.ai@connect.polyu.hk

The Hong Kong Polytechnic University
HKSAR, China

Yuni Lai

yunie.lai@connect.polyu.hk

The Hong Kong Polytechnic University
HKSAR, China

Kai Zhou

kaizhou@polyu.edu.hk

The Hong Kong Polytechnic University
HKSAR, China

ABSTRACT

Despite the tremendous success of graph neural networks in learning relational data, it has been widely investigated that graph neural networks are vulnerable to structural attacks on homophilic graphs. Motivated by this, a surge of robust models is crafted to enhance the adversarial robustness of graph neural networks on homophilic graphs. However, the vulnerability based on heterophilic graphs remains a mystery to us. To bridge this gap, in this paper, we start to explore the vulnerability of graph neural networks on heterophilic graphs and theoretically prove that the update of the negative classification loss is negatively correlated with the pairwise similarities based on the powered aggregated neighbor features. This theoretical proof explains the empirical observations that the graph attacker tends to connect dissimilar node pairs based on the similarities of neighbor features instead of ego features both on homophilic and heterophilic graphs. In this way, we novelly introduce a novel robust model termed **NSPGNN** which incorporates a dual-kNN graphs pipeline to supervise the neighbor-similarity-guided propagation. This propagation utilizes the low-pass filter to smooth the features of node pairs along the positive kNN graphs and the high-pass filter to discriminate the features of node pairs along the negative kNN graphs. Extensive experiments on both homophilic and heterophilic graphs validate the universal robustness of **NSPGNN** compared to the state-of-the-art methods.

KEYWORDS

Adversarial Graph Analysis, Graph Mining, Graph Machine Learning

ACM Reference Format:

Yulin Zhu, Yuni Lai, Xing Ai, and Kai Zhou. 2018. Universally Robust Graph Neural Networks by Preserving Neighbor Similarity. In *Proceedings of ACM Conference (Conference'17)*. ACM, New York, NY, USA, 12 pages. <https://doi.org/XXXXXXX.XXXXXXX>

Permission to make digital or hard copies of all or part of this work for personal or classroom use is granted without fee provided that copies are not made or distributed for profit or commercial advantage and that copies bear this notice and the full citation on the first page. Copyrights for components of this work owned by others than the author(s) must be honored. Abstracting with credit is permitted. To copy otherwise, or republish, to post on servers or to redistribute to lists, requires prior specific permission and/or a fee. Request permissions from permissions@acm.org.
Conference'17, July 2017, Washington, DC, USA

© 2018 Copyright held by the owner/author(s). Publication rights licensed to ACM.
ACM ISBN 978-1-4503-XXXX-X/18/06
<https://doi.org/XXXXXXX.XXXXXXX>

1 INTRODUCTION

The graph data ubiquitously appears in various domains such as biostatistics, finance and cryptocurrency [2, 33, 36, 39, 40]. Recently, the tremendous success of Graph Neural Networks (GNNs) has stimulated the wide applications of graph machine learning framework on node classification [10, 15], graph classification [16, 29] and link prediction [5, 30] etc. The powerful representation learning of GNN comes from the crafted propagation mechanism which is particularly suitable for tackling the structural data and highly relies on the homophily assumption [26] (connected nodes tend to share similar features). However, there are ubiquitous heterophilic graphs (connected nodes tend to share dissimilar features) that exist in the real world and the vanilla GNNs cannot handle them well [3, 4, 42]. Fortunately, plenty of GNN variants [3, 4, 7, 23, 42] endeavor to mitigate this problem by introducing some useful techniques such as ego- and neighbor-embeddings separation [42], aggregation with high-pass filter [3], concatenating with higher order neighbors' embeddings [4] etc. Those powerful techniques extend the application of the GNN framework and enrich the family of graph-based-deep-learning models.

Despite the tremendous success of GNNs, it has been widely explored that GNNs are vulnerable to graph structural attacks (adding or deleting a fraction of links to the clean graph) [37, 43–45]. In particular, the adversarial robustness of GNNs over homophilic graphs has been fully investigated [8, 13, 35, 38]. One of the most important observations is that the graph structural attacks tend to connect node pairs that are dissimilar and remove links that connect similar nodes [35]. Intuitively, adding inter-class links or deleting intra-class links will decrease the homophily level of the graph data and in turn, the message-passing operation will mix up the differentiation among different clusters and thus degrade the quality of node embeddings.

However, the above-mentioned observations fail to curve the adversarial robustness of GNNs over heterophilic graphs. For instance, Fig. 1 depicts the homophily ratios [42] (Referring to Sec. 3.1) and classification accuracies of GNN for Squirrel [28] dataset under different attacking scenarios. The results show that the graph attackers can still significantly degenerate the node classification performance of GNN for the heterophilic graph. However, in contrast to the homophilic graphs, the homophily ratio of the heterophilic graph increases after being attacked. These contradictions demonstrate that current robust models [13, 35, 38] fail to defend against

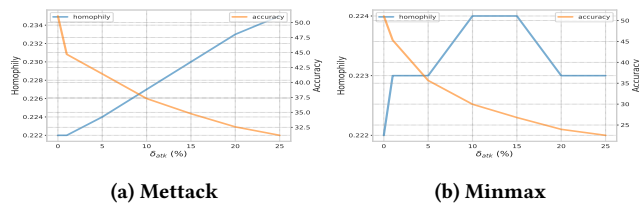


Figure 1: Homophily ratios and accuracies of the poisoned heterophilic graphs under different attacking scenarios.

the graph structural attacks for heterophilic graphs. In reality, most robust models rely on the similarities of ego features to mitigate the malicious effects caused by the graph attacker. However, for heterophilic graphs, the current robust techniques cannot tell apart malicious inter-class links from normal inter-class links and hence fail to prune the malicious effects on the poisoned graphs. Essentially, it is urgent to craft a novel technique to effectively pick out malicious effects of the graph data beyond ego features’ similarities.

To handle the above-mentioned problem, we propose a novel GNN framework termed Neighbor Similarity Preserving Graph Neural Network (**NSPGNN**) and start from a theoretical observation—the update of the attack loss (log-likelihood loss) $d\mathcal{L}_{atk}$ and the pairwise similarity matrix based on the τ -th powered aggregated neighbor features $A^\tau X$ are negatively correlated. Consequently, the graph attacker tends to connect the dissimilar node pairs based on the neighbor features. In other words, we extend the idea of the adversarial property from considering the similarities based on ego features to neighbor features. Affluent empirical studies in Fig. 2 support this finding and demonstrate that *malicious links are more likely to be such links that connect dissimilar node pairs based on $A^\tau X$ rather than X* . As a result, this insight can serve as malicious links detection and supervise the robust graph learning strategy.

Besides, we craft the dual-kNN graph pipelines to supervise the *neighbor-similarity-guided propagation* during training to obtain high-quality node embeddings. Specifically, we construct positive kNN graphs and negative kNN graphs based on the descending order and ascending order of the top- k similarity scores of $A^\tau X$ to contrastively supervise the graph convolutional operation to propagate node features while preserving the aggregated neighbor features consistency. More specifically, the structural information of the positive kNN graphs is implemented with a low-pass filter [34] to smooth the node’s features with its nearest neighbors according to the similarity scores. In sharp contrast to that, the structural information of the negative kNN graphs is implemented with high-pass filter [3, 23] to discriminate the node’s features with its farthest neighbors to preserve the aggregated node features’ similarity from an opposite perspective. In the sequel, the node embeddings obtained from low-pass filter and high-pass filter are fused to form the final node embeddings and fed into the classification loss.

In summary, the main contributions are three folds:

- We both theoretically and empirically illustrate that preserving the aggregated neighbors’ similarity can detect the

potential malicious effects and universally enhance the adversarial robustness of GNNs.

- We propose a universal robust GNN framework—**NSPGNN** to preserve the aggregated neighbors’ similarity by introducing a dual-kNN graphs pipeline to contrastively supervise the neighbor-similarity-guided propagation.
- **NSPGNN** competitively outperforms other baselines both on homophilic and heterophilic graphs under different adversarial environments.

2 RELATED WORKS

2.1 GNN for Heterophilic Graphs

To date, graph neural networks have achieved tremendous success in tackling the semi-supervised learning problem for relational data. However, there exists a limitation of the vanilla GNNs—the aggregation mechanism of the graph convolutional operation is specially crafted for the homophilic graphs, which narrows the application of GNN in the real world. Fortunately, a series of GNN variants have been proposed to bypass this limitation and can handle heterophilic graphs. For instance, H2GCN [42] crafted three vital designs: ego- and neighbor-embedding separation, higher-order neighborhoods and a combination of intermediate representations to enhance the expressive power of GNN for heterophilic graphs. FAGNN [3] can adaptively change the proportion of low-frequency and high-frequency signals to efficiently mine the semantic and structural information of heterophilic graphs. GPRGNN [4] introduced the generalized PageRank GNN framework to adaptively assign the GPR weights to jointly optimize node features and topological information extraction. GBKGNN [7] adopts a bi-kernel for feature extraction and a selection gate to enhance the representation learning of GNN over uneven homophily levels of heterophilic graphs. BMGNN [12] incorporates block modeling information into the aggregation process, which can help GNN to aggregate information from neighbors with distinct homophily degrees. ACMGNN [23] proposes the adaptive channel mixing framework adaptively exploits aggregation, diversification and identity channels node-wisely to extract richer localized information for diverse node heterophily situations.

2.2 Robust GNNs

It has been widely explored that GNNs are vulnerable to graph structural attacks [37, 43–45] since the aggregation mechanism of the graph convolutional layer highly relies on topology information of the relational data. To address this problem, a battery of defense methods against the graph structural attacks has been investigated. For example, GCNJaccard [35] prunes the malicious links via the Jaccard index on the node attributes. GNNGUARD [38] removes the malicious links during training by considering the cosine similarity of node features. ProGNN [13] learns a new dense adjacency matrix and GNN simultaneously by penalizing three graph properties: matrix rank, the nuclear norm of the adjacency matrix and feature smoothness. However, the above-mentioned robust models are highly reliant on the homophily assumption and may not be suitable for boosting the robustness of GNN over heterophilic graphs. Alternatively, GARNET [6] learns a new reduced-rank graph topology via spectral graph embedding and probabilistic graphical model

to enhance the GNN's robustness. It can enhance the robustness of GNNs over heterophilic graphs since it does not depend on the homophily assumption. However, the strong assumption of the Gaussian graphical model will mitigate the quality of its base graph construction.

3 PRELIMINARIES

3.1 Homophily and Heterophily

The diversification of the homophilic graph and heterophilic graph mainly comes from the matching degree between the target node and its surroundings. It is worth noting that recent literature [3, 4, 7, 42] uses the following metric to measure the homophily degree of the graph data:

$$\mathcal{H}(G) = \frac{|\{e_{uv} \in \mathcal{E}, y_u = y_v\}|}{|\mathcal{E}|}, \quad (1)$$

where \mathcal{E} is the edge set, y_u represents the label for node u .

3.2 Semi-supervised Node Classification

The input is an attributed graph $G = \{\mathcal{V}, \mathbf{X}, \mathbf{A}, \mathcal{Y}\}$, where $\mathbf{X} \in \mathbb{R}^{N \times p}$ is the nodal attribute matrix, N is the node number, $\mathbf{A} \in \{0, 1\}^{N \times N}$ is the adjacency matrix where $A_{uv} = 1$ represents that the node u is connected with node v and vice versa, $\{\mathcal{Y}_u\}_{u=1}^N$ is the label for node u . The node set \mathcal{V} is usually partitioned into training set \mathcal{V}_{tr} , validation set \mathcal{V}_{val} and testing set \mathcal{V}_{te} respectively. The most representative graph-based deep learning models are GNN and its variants. In particular, the GNN is formulated as an encoder $f_{\mathcal{W}}(\mathbf{X}, \mathbf{A}) \rightarrow \mathbf{Z}$, which maps the complex structural data to an Euclidean embedding space. Specially, there are two common graph filters [3, 23, 34] for node representation learning:

$$\text{low-pass: } \mathbf{Z} = \sigma(\hat{\mathbf{A}}\mathbf{X}\mathbf{W}), \quad \text{high-pass: } \mathbf{Z} = \sigma((\mathbf{I} - \hat{\mathbf{A}})\mathbf{X}\mathbf{W}), \quad (2)$$

where $\hat{\mathbf{A}} = \tilde{\mathbf{D}}^{-\frac{1}{2}} \tilde{\mathbf{A}} \tilde{\mathbf{D}}^{-\frac{1}{2}}$, $\tilde{\mathbf{A}} = \mathbf{A} + \mathbf{I}$, $\tilde{\mathbf{D}} = \text{Diag}\{d_{ii}\}_{i=1}^N$, $d_{ii} = \sum_{j=1}^N A_{ij}$.

3.3 Graph Structural Attacks

It has been widely explored that GNNs are vulnerable to graph structural attacks [18, 37, 43–45]. To this end, the graph attacker aims at manipulating the clean graph's structure \mathbf{A} with limited budgets to minimize the predicting accuracy on the unlabeled nodes without significantly altering the graph property such as node degree distribution [43]. Mathematically, the graph structural attacks can be formulated as a discrete bi-level optimization problem:

$$\mathbf{A}^p = \arg \min_{\mathbf{A}} \mathcal{L}_{atk} = -\mathcal{L}_{NLL}(\mathbf{X}, \mathbf{A}, \mathbf{W}^*, \mathcal{Y}, \mathcal{V}_{te}), \quad (3a)$$

$$\text{s.t. } \mathbf{W}^* = \arg \min_{\mathbf{W}} \mathcal{L}_{NLL}(\mathbf{X}, \mathbf{A}, \mathbf{W}, \mathcal{Y}, \mathcal{V}_{tr}), \quad \|\mathbf{A}^p - \mathbf{A}\| \leq B. \quad (3b)$$

4 VULNERABILITY ANALYSIS

We start by investigating the vulnerability of GNNs over the heterophilic graphs. Vanilla robust models rely on the similarities of ego features to detect potential malicious links from benign ones [13, 35, 38] based on the poisoned homophilic graphs. However, this strategy may not be suitable for enhancing the adversarial robustness of GNNs under the heterophily scenario. For instance, in Fig. 2a and 2d, unlike the homophilic graphs, the density of the similarities of ego features fail to tell apart malicious links from

benign ones for heterophilic graphs. As a result, all the current robust GNN models based on the homophily assumption cannot improve the node classification performances for poisoned heterophilic graphs. Intuitively, there already exists a large proportion of benign heterophilic links (links connecting dissimilar node pairs) in the poisoned heterophilic graphs and the vanilla strategy cannot distinguish the malicious heterophilic links from the benign heterophilic links. Hence, the main challenge is to search for a new strategy to differentiate malicious heterophilic links from benign ones beyond the similarities of ego features.

4.1 Analysis of Attack Loss

In order to theoretically analyze the rationale behind the tremendous effectiveness of the graph structural attacks [37, 45] so as to provide a comprehensive explanation of the failure of GNN on the poisoned graphs, we first begin with investigating the update of the attack loss, i.e., $d\mathcal{L}_{atk}$ defined in Eqn. 3a since a common way to determine the structural perturbations is to measure the magnitude of the gradient information such as Mettack [45]. Hence, the exploration of the relationship between $d\mathcal{L}_{atk}$ and the information of the graph data such as the topology information \mathbf{A} and the semantic information \mathbf{X} may unveil the attack preferences on the topology space. In turn, the defender can craft a new strategy to boost the GNN's robustness according to this prior knowledge. We consider the simple SGC [34] as our victim model since it is usually considered the surrogate model for graph structural attacks. The SGC model is formulated as:

$$\mathbf{S} = \text{softmax}(\mathbf{Z}) = \text{softmax}(\hat{\mathbf{A}}^\tau \mathbf{X}\mathbf{W}), \quad (4)$$

where τ is the number of graph convolutional layers. The attacker's goal is to introduce structural poisons to minimize the attack loss \mathcal{L}_{atk} . We delve into the update of the attack loss of the SGC model and obtain the following theoretical observation:

LEMMA 1. *The gradient of the softmax $\mathbf{S}_i = \frac{\exp(\mathbf{Z}_i)}{\sum_j \exp(\mathbf{Z}_j)}$ is $\nabla_{\mathbf{Z}_j} \mathbf{S}_i = \mathbf{S}_i(1\{i=j\} - \mathbf{S}_i)$.*

THEOREM 2. *The magnitude of the update of the attack loss $d\mathcal{L}_{atk}$ is negatively related to the nodes' aggregated feature similarity matrix $\mathbf{K} = \mathbf{A}^\tau \mathbf{X}(\mathbf{A}^\tau \mathbf{X})^\top$.*

PROOF. In the inner loop of the attack objective defined in Eqn. 3, we have

$$d\mathbf{Z} = \hat{\mathbf{A}}^\tau \mathbf{X} d\mathbf{W} = \hat{\mathbf{A}}^\tau \mathbf{X} \cdot \gamma \nabla_{\mathbf{W}} \mathcal{L}_{nll} = \hat{\mathbf{A}}^\tau \mathbf{X} \cdot \gamma \nabla_{\mathbf{Z}} \mathcal{L}_{nll} \nabla_{\mathbf{W}} \mathbf{Z}. \quad (5)$$

On the other hand, we have:

$$\nabla_{\mathbf{Z}_i} \mathcal{L}_{nll} = \nabla_{\mathbf{Z}_i} \left(- \sum_{c=1}^C Y_{ic} \log S_{ic} \right) = - \sum_{c=1}^C \frac{Y_{ic}}{S_{ic}} \nabla_{\mathbf{Z}_i} S_{ic}, \quad (6)$$

However, from Lemma. 1 we can have:

$$[\nabla_{\mathbf{Z}_{ic'}} S_{ic}]_{c'=1}^C = [S_{ic}(1\{c=c'\} - S_{ic})]_{c'=1}^C, \quad (7)$$

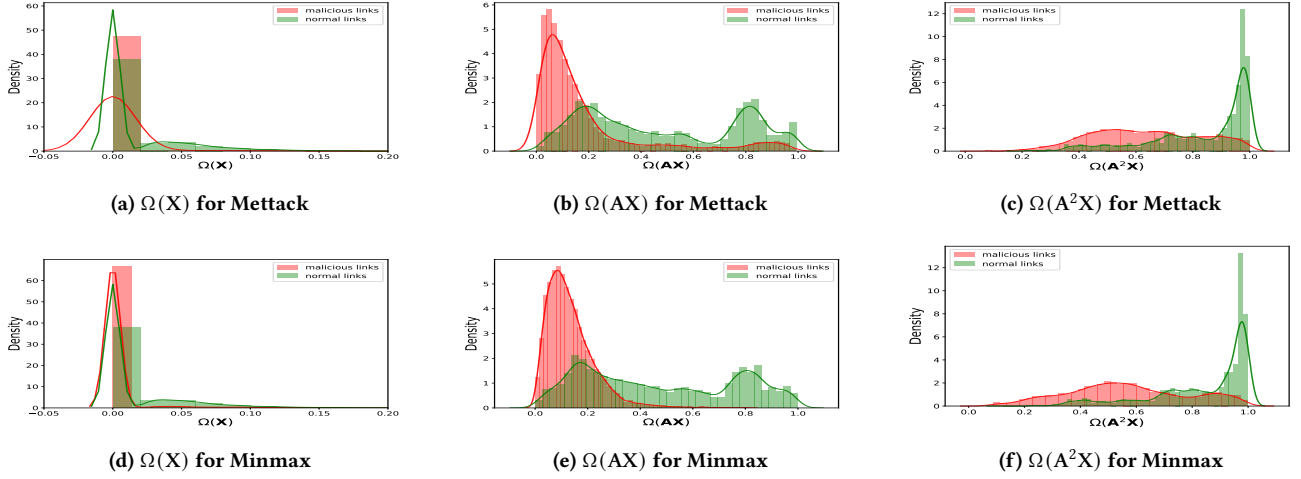


Figure 2: Density plots of $\Omega(X)$, $\Omega(AX)$, $\Omega(A^2X)$ between benign links and malicious links on Chameleon.

Then,

$$\begin{aligned}
 [\nabla_{Z_{ic'}} \mathcal{L}_{nll}]_{c'=1}^C &= -\left[\sum_{c=1}^C \frac{Y_{ic}}{S_{ic}} S_{ic} (1\{c=c'\} - S_{ic}) \right]_{c'=1}^C \\
 &= -\left[\sum_{c=1}^C Y_{ic} (1\{c=c'\} - S_{ic}) \right]_{c'=1}^C \quad (8) \\
 &= [S_{ic'} - Y_{ic'}]_{c'=1}^C.
 \end{aligned}$$

In matrix formation, we have $\nabla_{Z_i} \mathcal{L}_{nll} = S_i - Y_i$. Also, the gradient of Z w.r.t W is $\nabla_W Z = (\hat{A}^\tau X)^\top$. Hence, we have:

$$\begin{aligned}
 dZ|_{Z=Z^*} &\propto \hat{A}^\tau X (\hat{A}^\tau X)^\top (S^* - Y), \\
 d\mathcal{L}_{atk} &= -\nabla_Z \mathcal{L}_{nll} dZ \propto -\text{Tr}((S^* - Y)^\top \hat{A}^\tau X (\hat{A}^\tau X)^\top (S^* - Y)) \\
 &= -\text{Tr}((S^* - Y)^\top D^{-1} A^\tau X (D^{-1} A^\tau X)^\top (S^* - Y)) \\
 &= -\text{Tr}(\Delta A^\tau X (A^\tau X)^\top \Delta^\top) = -\sum_{i,j=1}^N K_{ij} \delta_i \delta_j^\top, \quad (9)
 \end{aligned}$$

where $K = A^\tau X (A^\tau X)^\top$ is the kernel matrix based on $A^\tau X$, δ_i is the i -th vector of $\Delta = (S^* - Y)^\top D^{-1}$. \square

Theorem. 2 illustrates that the magnitude of the update of the attack loss is negatively related to the similarity matrix $K = A^\tau X (A^\tau X)^\top$. Hence, the graph attacker tends to connect the node pair (u, v) with a low value of the similarity score K_{uv} to predominantly influence the attack loss \mathcal{L}_{atk} as much as possible.

4.2 Exploring Attack Preference

Theorem. 2 verifies that connecting dissimilar node pairs based on the similarity matrix K may provide a larger magnitude of the update of the attack loss and thus significantly influence the node classification performance. In this section, we implement a series of empirical studies to elaborate more on this issue. Without loss

of generalizability, we define the similarity matrix as:

$$\Omega(A^\tau X)[i, j] = \frac{A^\tau X[i]^\top \cdot A^\tau X[j]}{\|A^\tau X[i]\| \cdot \|A^\tau X[j]\|}, \quad (10)$$

where τ is the power of a matrix. It is worth noting that vanilla robust models use the similarity of ego features, i.e., $\Omega(X)$ to curve the attack preference of the graph attacker. More specifically, the graph attacker tends to connect dissimilar node pairs based on $\Omega(X)$. We take Chameleon [28] as examples to observe the attack preference of the graph attacker for heterophilic graphs. We first utilize Mettack [45] and MinMax [37] as two representative graph structural attacks on Chameleon. Then, we report the cosine similarity score [31] based on ego features $\Omega(X)$ and one-hop neighbors features $\Omega(AX)$ and two-hop neighbors features $\Omega(A^2X)$ for benign links and malicious links in Fig. 2. It is observed that for the heterophilic graph, $\Omega(X)$ cannot differentiate the malicious links from benign links since their densities are similar. However, there exists a significant difference between the density of $\Omega(AX)$ and $\Omega(A^2X)$ for benign links and malicious links and the mean values for malicious links are far less than benign links. Moreover, we want to emphasize that the attack preference based on $\Omega(A^\tau X)$ also works for homophilic graphs since Theorem. 2 is independent of the homophily ratio of the graph data. We will provide more experiments to verify this issue in a later section.

4.3 Over-smoothing of $\Omega(A^\tau X)$

The choices of the graph convolutional layer τ still remain a problem. In particular, Fig. 3 provides the density of the similarity scores for higher-order layers. The phenomena demonstrate that high-order $\Omega(A^\tau X)$ cannot tell apart the malicious and benign links since the two densities are mixed up. This is caused by the over-smoothing [19] issue. Specifically, repeatedly applying the aggregation operation may mix the attributes of nodes from different clusters and make them indistinguishable. Hence, it is vital to choose a level of depth τ for crafting an efficient robust model. Without loss of generality, we choose $\tau = 1$ and 2 in the model setting.

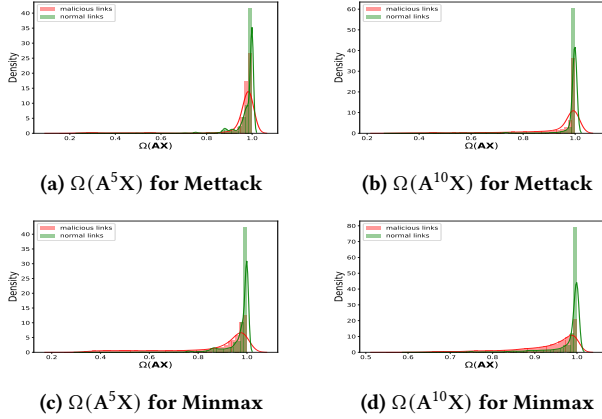


Figure 3: Density plots of $\Omega(\mathbf{A}^5\mathbf{X})$ and $\Omega(\mathbf{A}^{10}\mathbf{X})$ between benign links and malicious links for Mettack and Minmax.

5 PROPOSED MODEL: NSPGNN

5.1 Framework Overview

The overall architecture of the proposed NSPGNN is depicted in Fig. 4. The goal of NSPGNN is to aggregate the node features along the path which can preserve the neighbor’s similarity $\Omega(\mathbf{A}^\tau\mathbf{X})$. First, NSPGNN constructs two positive k -nearest neighbor (kNN) graphs [27] \mathbf{A}^{kNN_1} and \mathbf{A}^{kNN_2} and two negative kNN graphs (to be detailed later) \mathbf{A}^{nkNN_1} and \mathbf{A}^{nkNN_2} based on the one-hop and two-hop aggregated feature matrix $\mathbf{A}\mathbf{X}$ and $\mathbf{A}^2\mathbf{X}$. Then, the node features are propagated adaptively from \mathbf{A}^{kNN_1} , \mathbf{A}^{kNN_2} , \mathbf{A}^{nkNN_1} and \mathbf{A}^{nkNN_2} with the learnable weights to balance the relative importance. Especially, the node features are aggregated with the low-pass filter [34] ($\hat{\mathbf{A}}^{kNN_1}$ and $\hat{\mathbf{A}}^{kNN_2}$) to push the embeddings of node pairs with high similarity score similar and aggregated with the high-pass filter [23] ($\mathbf{I}-\hat{\mathbf{A}}^{nkNN_1}$ and $\mathbf{I}-\hat{\mathbf{A}}^{nkNN_2}$) simultaneously to push the embeddings of node pairs with low similarity score dissimilar.

5.2 Dual-kNN Graphs Construction

As previously mentioned in Sec. 4, it has been theoretically and empirically illustrated that the vulnerability of the GNN framework is highly dependent on the similarities of the neighbors’ features, i.e., $\Omega(\mathbf{A}^\tau\mathbf{X})$. To universally enhance the adversarial robustness of the GNN framework over homophilic and heterophilic graphs, we endeavor to craft a robust GNN framework guided by the neighbor similarity information to get rid of the malicious effects in the poisoned graphs. To this end, we construct two positive kNN graphs \mathbf{A}^{kNN_1} and \mathbf{A}^{kNN_2} to capture the high-level similarity information and two negative kNN graphs \mathbf{A}^{nkNN_1} and \mathbf{A}^{nkNN_2} to serve as its counterpart. As a result, propagating along the two distinct structure information (high similarity v.s. low similarity) can contrast with each other and double-preserve the neighbor similarity.

5.2.1 Positive kNN Graphs. To incorporate the neighbor similarity information into the GNN framework, we first propose to encode

the high-level similarity information of the prerequisite similarity matrix $\Omega(\mathbf{A}^\tau\mathbf{X})$ into the structural information. The crafted structural information can serve as the positive path to smooth the features of node pairs with high similarity scores. For constructing the positive kNN graphs, we transform the features $\mathbf{A}^\tau\mathbf{X}$ into a topology by generating a kNN graph based on $\Omega(\mathbf{A}^\tau\mathbf{X})$ (presented in Eqn. 10). In the sequel, we pick out the top- k nearest neighbors for each node to construct the corresponding kNN graph, i.e.,

$$\mathbf{A}^{kNN_\tau}[u] \in \text{Argsort_Desc}_{v \in \mathcal{V} \setminus u} \frac{\mathbf{A}^\tau\mathbf{X}[u]^\top \cdot \mathbf{A}^\tau\mathbf{X}[v]}{\|\mathbf{A}^\tau\mathbf{X}[u]\| \cdot \|\mathbf{A}^\tau\mathbf{X}[v]\|}, \tau = 1, 2, \quad (11)$$

where $\text{Argsort_Desc}(\cdot)$ represents picking out indices of samples with descending order. Consequently, the target node in the positive graph \mathbf{A}^{kNN_τ} will connect with other similar nodes based on $\Omega(\mathbf{A}^\tau\mathbf{X})$.

5.2.2 Negative kNN Graphs. The limitation of the positive kNN graphs is that they only contain information on high-value similarity scores and omit the dissimilarity information between node pairs. To tackle this problem, we contrastively introduce negative kNN graphs \mathbf{A}^{nkNN_τ} to encode the low-level similarity information into the structure information to supervise propagation:

$$\mathbf{A}^{nkNN_\tau}[u] \in \text{Argsort_Asc}_{v \in \mathcal{V} \setminus u} \frac{\mathbf{A}^\tau\mathbf{X}[u]^\top \cdot \mathbf{A}^\tau\mathbf{X}[v]}{\|\mathbf{A}^\tau\mathbf{X}[u]\| \cdot \|\mathbf{A}^\tau\mathbf{X}[v]\|}, \tau = 1, 2, \quad (12)$$

where $\text{Argsort_Asc}(\cdot)$ represents picking out indices of samples with ascending order. In this way, the negative graphs \mathbf{A}^{nkNN_τ} can capture the extremely dissimilar information and serve as the counterpart against the positive graphs.

5.3 Neighbor-Similarity-Guided Propagation

After the dual-kNN graphs construction phase, it is important to determine the best choices for the aggregation mechanism to propagate node features while preserving the neighbor similarity effectively. Toward this end, we introduce an adaptive neighbor-similarity-guided propagation mechanism. The formal form of the information flow for the node representation learning is:

$$[\alpha_1^{(l)}, \alpha_2^{(l)}] = \sigma(\mathbf{H}^{(l-1)}\mathbf{W}_m^{(l)} + \mathbf{b}_m^{(l)}), \quad (13a)$$

$$[\beta_1^{(l)}, \beta_2^{(l)}] = \sigma(\mathbf{H}^{(l-1)}\mathbf{W}_n^{(l)} + \mathbf{b}_n^{(l)}), \quad (13b)$$

$$\hat{\mathbf{A}}^{kNN_\tau} = (\tilde{\mathbf{D}}^{kNN_\tau})^{-\frac{1}{2}} \tilde{\mathbf{A}}^{kNN_\tau} (\tilde{\mathbf{D}}^{kNN_\tau})^{-\frac{1}{2}}, \tau = 1, 2, \quad (13c)$$

$$\hat{\mathbf{A}}^{nkNN_\tau} = (\tilde{\mathbf{D}}^{nkNN_\tau})^{-\frac{1}{2}} \tilde{\mathbf{A}}^{nkNN_\tau} (\tilde{\mathbf{D}}^{nkNN_\tau})^{-\frac{1}{2}}, \tau = 1, 2, \quad (13d)$$

$$\hat{\mathbf{A}}^p{}^{(l)} = \alpha_1^{(l)} \odot \hat{\mathbf{A}}^{kNN_1} + \alpha_2^{(l)} \odot \hat{\mathbf{A}}^{kNN_2}, \quad (13e)$$

$$\hat{\mathbf{A}}^n{}^{(l)} = \beta_1^{(l)} \odot \hat{\mathbf{A}}^{nkNN_1} + \beta_2^{(l)} \odot \hat{\mathbf{A}}^{nkNN_2}, \quad (13f)$$

$$\mathbf{H}^{(l)} = \sigma(\mathbf{H}^{(l-1)}\mathbf{W}_s^{(l)}) + \underbrace{\hat{\mathbf{A}}^p{}^{(l)}\mathbf{H}^{(l-1)}\mathbf{W}_o^{(l)}}_{\text{Low-pass filter}} + \underbrace{(\mathbf{I}-\hat{\mathbf{A}}^n{}^{(l)})\mathbf{H}^{(l-1)}\mathbf{W}_d^{(l)}}_{\text{High-pass filter}}, \quad (13g)$$

where $\tilde{\mathbf{A}}^{kNN_\tau} = \mathbf{A}^{kNN_\tau} + \mathbf{I}$ and $\tilde{\mathbf{A}}^{nkNN_\tau} = \mathbf{A}^{nkNN_\tau} + \mathbf{I}$, $\tau = 1, 2$, $\mathbf{H}^{(0)} = \mathbf{X}$, $\sigma(\cdot)$ is the activation function such as ReLU [1].

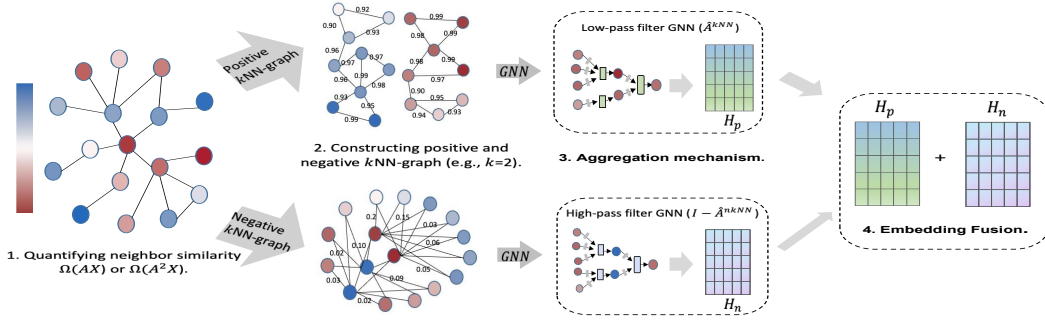


Figure 4: An overview of NSPGNN.

In this process, we train the learnable weight matrix $\alpha_1^{(l)}$, $\alpha_2^{(l)}$, $\beta_1^{(l)}$ and $\beta_2^{(l)}$ at each layer by implementing a multi-layer perceptron (MLP [11]) on the nodal feature matrix $\mathbf{H}^{(l-1)}$ to adaptively balance the relative importance between the one-hop and two-hop neighbor similarity information for positive kNN graphs and negative kNN graphs. Next, we propagate the node features along the new structures $\hat{\mathbf{A}}^p^{(l)}$ with a low-pass filter to smooth the features of similar node pairs. Alternatively, the node features are aggregated along the negative structure $\hat{\mathbf{A}}^n^{(l)}$ with a high-pass filter to enlarge the distance of the features of dissimilar node pairs. In the meanwhile, we assign different weight matrices for ego-embeddings $\mathbf{H}^{(l-1)}$ and neighbor-embeddings obtained from low-pass and high-pass filters to let the model determine the relative importance of self-loops for graph representation learning. It is worth noting that \odot denotes the operation to multiply the i -th element vector with the i -th row of a matrix. Finally, the three parties (ego-embeddings $\mathbf{H}^{(l-1)}\mathbf{W}_s^{(l)}$, low-pass embeddings $\hat{\mathbf{A}}^p^{(l)}\mathbf{H}^{(l-1)}\mathbf{W}_o^{(l)}$ and high-pass embeddings $(\mathbf{I} - \hat{\mathbf{A}}^n^{(l)})\mathbf{H}^{(l-1)}\mathbf{W}_d^{(l)}$) together determine the final node embeddings for semi-supervised node classification.

6 EXPERIMENTS

In this section, we aim to answer the following questions:

- **RQ1:** What are the robust performances of NSPGNN compared to baselines on homophilic and heterophilic graphs?
- **RQ2:** How do different modules impact model performance?
- **RQ3:** What are the influences of varying hyperparameters?

6.1 Experiment Settings

6.1.1 Dataset. In this paper, we mainly investigate the adversarial robustness of GNN framework against the graph structural attacks. Thus, we conduct experiments on three typical heterophilic graphs: Chameleon, Squirrel and Crocodile¹ [28] and three homophilic graphs: Cora, CiteSeer [25] and Photo [24].

6.1.2 Setup. We use *Pytorch-Geometric* [9] to preprocess the six graph datasets and implement robust models, i.e., GCN-Jaccard [35], ProGNN [13] on *DeepRobust* [20], and GNNGUARD [38], RGCN [41], AirGNN [21] and ElasticGNN [22] on GreatX [17]. We implement GNN variants crafted for heterophilic graphs (HGNNs) like GPRGNN [4],

¹Mettack fails to attack Crocodile because of cuda out of memory.

FAGNN [3], GBKGNN [7], BMGCN [12] and ACMGNN [23], GARNET [6] based on their source code. We evaluate the robustness of GNNs over homophilic and heterophilic graphs on the semi-supervised node classification task and conduct 10 individual experiments with varying seeds and report the mean and standard error of the test accuracies for fair comparisons. We consider two typical graph structural attacks: Mettack [45] and Minmax [37] with the attacking power $\delta_{atk} = \{1\%, 5\%, 10\%, 15\%, 20\%, 25\%\}$, which represents the proportion of the modified links over the link set \mathcal{E} . We tune the hyperparameters k_1 and k_2 from the set $\{1, 5, 10, 15, 20, 25, 30\}$ and determine the best choices based on the validation accuracy. We train 500 epochs in all experiments using the Adam [14] optimizer with a learning rate of 0.01 for all the models.

6.2 Robustness over Heterophilic Graphs

6.2.1 Defense Against Mettack. The results in Tab. 1 present the semi-supervised node classification performances of NSPGNN and other HGNN baselines over three heterophilic graphs under Mettack with varying attacking powers. It is worth noting that NSPGNN **w.o.** is the ablation of the proposed model where we omit the negative kNN graphs construction. We have the following three observations: **1)** The proposed model NSPGNN and its ablation consistently outperform other HGNNs by a large margin. For example, NSPGNN outperforms the second-best performances around 24.72%, 27.12%, 29.88%, 32.99%, 34.31%, 33.71% for Squirrel dataset with attacking power δ_{atk} equal to 1%, 5%, 10%, 15%, 20%, 25% respectively. These phenomenons indicate that preserving the neighbor similarity can effectively defend against Mettack on heterophilic graphs. **2)** Compared to its ablation, NSPGNN achieves slightly better node classification accuracies for most cases, which demonstrates that the negative kNN graphs play an important role when supervising the neighbor-similarity-guided propagation. **3)** the performance gains between NSPGNN **w.o.** and the second-best performances are larger than the performance gains between NSPGNN **w.o.** and NSPGNN indicates that propagation with positive kNN graphs is far more effective than propagation with negative kNN graphs. It makes sense since preserving the high-similarity information will likely prune the malicious links and thus enhance the adversarial robustness of GNNs.

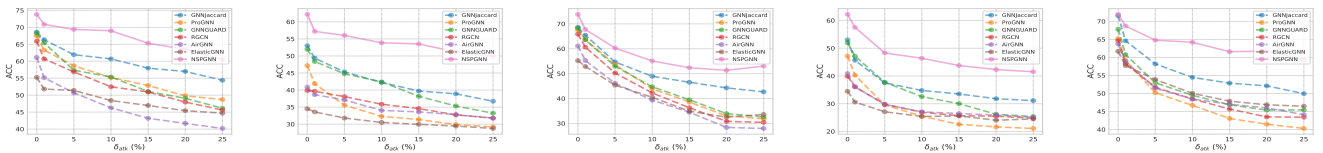
In the meanwhile, we also compare the proposed model with other robust model benchmarks against Mettack on heterophilic graphs in Fig. 5a and 5b. It is observed that NSPGNN consistently

Table 1: Robust performances of GNNs over heterophilic graphs against Mettack.

Dataset	δ_{atk}	GPRGNN	FAGNN	H2GCN	GBKGN	BMGCN	ACMGNN	GARNET	NSPGNN w.o.	NSPGNN
Chameleon	1%	64.04 (0.98)	67.28 (0.54)	59.41 (0.95)	64.43 (1.00)	65.79 (0.95)	64.32 (1.25)	64.63 (1.02)	70.59 (0.99)	70.88 (1.00)
	5%	62.87 (0.96)	62.76 (0.62)	57.06 (0.91)	57.00 (0.92)	62.17 (0.85)	60.44 (0.81)	60.88 (1.01)	70.02 (1.01)	69.39 (0.74)
	10%	59.34 (0.96)	56.56 (0.87)	54.43 (0.80)	54.34 (1.12)	59.82 (1.06)	58.62 (1.29)	59.04 (0.93)	67.54 (0.88)	68.99 (0.87)
	15%	56.91 (1.29)	55.22 (1.06)	54.04 (1.00)	51.10 (1.34)	56.62 (0.86)	56.56 (1.10)	56.54 (1.19)	64.78 (0.74)	65.31 (1.17)
	20%	54.21 (0.73)	52.46 (0.66)	53.62 (1.58)	49.43 (1.08)	55.66 (0.91)	55.15 (1.43)	55.09 (1.00)	63.14 (0.79)	63.53 (0.89)
	25%	52.32 (0.66)	50.48 (0.59)	52.50 (1.01)	47.41 (0.90)	54.69 (0.94)	54.36 (1.09)	54.84 (1.12)	60.46 (0.77)	60.53 (0.62)
Squirrel	1%	40.75 (2.00)	46.83 (3.19)	33.28 (1.00)	50.56 (1.19)	44.61 (0.94)	48.06 (1.06)	45.87 (1.20)	55.80 (0.93)	57.21 (0.92)
	5%	39.42 (1.20)	41.99 (1.76)	33.06 (1.13)	46.11 (0.92)	42.33 (0.77)	46.41 (1.62)	44.07 (1.09)	52.91 (0.79)	56.02 (0.54)
	10%	35.28 (1.21)	38.13 (1.61)	33.64 (1.05)	40.98 (2.61)	40.89 (0.81)	42.78 (0.55)	41.46 (1.11)	51.83 (0.63)	53.85 (1.10)
	15%	32.90 (0.83)	36.25 (1.00)	32.83 (0.86)	37.71 (1.57)	39.28 (0.38)	40.74 (1.31)	40.25 (1.25)	51.24 (0.47)	53.53 (0.92)
	20%	31.27 (0.65)	34.20 (1.81)	32.26 (1.27)	34.71 (2.06)	38.27 (0.71)	38.77 (1.17)	38.12 (1.03)	49.98 (0.78)	51.20 (0.72)
	25%	30.18 (1.26)	32.86 (2.58)	32.65 (1.20)	32.79 (1.21)	36.77 (0.69)	37.45 (1.40)	37.38 (0.84)	48.60 (0.81)	49.98 (0.80)

Table 2: Robust performances of GNNs over heterophilic graphs against Minmax.

Dataset	δ_{atk}	GPRGNN	FAGNN	H2GCN	GBKGN	BMGCN	ACMGNN	GARNET	NSPGNN w.o.	NSPGNN
Chameleon	Clean	71.01 (1.12)	69.89 (0.63)	61.73 (0.80)	69.39 (0.67)	67.90 (1.07)	68.20 (1.20)	67.74 (1.10)	72.87 (0.91)	73.84 (0.56)
	1%	61.47 (0.93)	61.40 (2.46)	58.75 (1.15)	64.01 (0.56)	63.47 (0.87)	64.30 (0.92)	61.75 (0.93)	67.71 (0.68)	67.76 (1.00)
	5%	51.71 (0.65)	50.72 (1.11)	51.40 (1.05)	52.06 (0.57)	52.59 (0.73)	53.05 (1.60)	57.92 (0.98)	58.31 (0.67)	60.29 (0.58)
	10%	46.29 (0.61)	43.77 (1.18)	47.32 (1.01)	44.85 (0.74)	47.24 (0.96)	48.07 (0.74)	51.56 (0.89)	55.64 (0.82)	55.11 (0.78)
	15%	43.20 (0.89)	39.41 (1.54)	43.88 (1.44)	39.71 (0.65)	44.10 (0.97)	44.39 (1.19)	46.69 (1.07)	52.01 (1.09)	52.39 (1.06)
	20%	39.67 (0.78)	35.39 (1.07)	41.16 (1.64)	33.25 (0.62)	43.38 (0.99)	44.43 (1.52)	48.89 (0.78)	51.40 (1.76)	51.34 (1.04)
	25%	38.38 (0.51)	34.45 (1.40)	41.38 (1.43)	32.94 (0.39)	43.82 (1.11)	43.55 (2.11)	47.79 (1.29)	51.56 (1.16)	53.05 (1.45)
Squirrel	Clean	51.30 (1.06)	52.62 (0.57)	34.39 (0.60)	53.68 (0.77)	47.78 (0.61)	51.21 (1.33)	47.82 (0.92)	59.90 (0.63)	62.21 (0.69)
	1%	42.46 (0.65)	43.22 (0.61)	29.49 (2.23)	48.61 (0.63)	40.65 (0.66)	44.10 (1.23)	42.60 (0.81)	55.69 (1.00)	57.52 (0.68)
	5%	34.52 (1.20)	33.50 (0.98)	28.17 (2.98)	38.70 (0.59)	33.14 (0.49)	36.09 (0.58)	36.50 (0.80)	45.38 (0.62)	48.32 (0.86)
	10%	32.92 (1.24)	30.21 (1.05)	29.06 (1.30)	33.15 (0.81)	31.98 (0.73)	33.80 (0.93)	34.69 (0.34)	43.51 (0.96)	46.37 (0.69)
	15%	32.41 (1.19)	27.80 (0.94)	27.93 (2.26)	30.30 (0.54)	32.04 (0.57)	34.47 (0.82)	34.89 (1.08)	40.76 (0.67)	43.77 (0.62)
	25%	31.05 (2.34)	25.14 (1.05)	28.61 (1.61)	26.95 (0.85)	30.71 (0.74)	32.73 (1.41)	33.54 (0.57)	40.18 (0.63)	42.31 (0.49)
Crocodile	Clean	63.18 (0.31)	66.54 (0.37)	54.71 (3.63)	69.66 (0.58)	69.42 (0.46)	69.82 (0.78)	68.53 (0.44)	71.85 (0.60)	71.96 (0.93)
	1%	57.50 (0.28)	61.13 (0.51)	54.40 (2.48)	62.32 (0.58)	63.63 (0.28)	62.97 (0.76)	64.50 (0.27)	68.75 (0.46)	68.72 (0.45)
	5%	51.50 (0.37)	55.57 (0.40)	53.46 (2.32)	53.58 (0.29)	58.92 (1.31)	57.76 (1.44)	62.51 (0.62)	64.76 (0.53)	64.78 (0.45)
	10%	47.96 (0.38)	52.72 (0.49)	46.11 (2.40)	49.71 (0.50)	55.71 (0.47)	57.82 (1.73)	59.52 (0.59)	63.28 (0.58)	64.20 (0.40)
	15%	46.54 (0.38)	50.59 (0.47)	43.01 (0.27)	47.46 (0.66)	53.68 (0.47)	55.84 (0.89)	58.52 (1.07)	59.32 (0.56)	61.58 (0.54)
	25%	45.66 (0.58)	49.99 (0.42)	42.88 (0.25)	46.17 (0.67)	52.99 (0.44)	56.27 (1.25)	60.29 (0.63)	60.32 (0.79)	61.75 (0.86)

**(a) Chameleon for Mettack (b) Squirrel for Mettack (c) Chameleon for Minmax (d) Squirrel for Minmax (e) Crocodile for Minmax****Figure 5: Accuracies of robust models against graph structural attacks over heterophilic graphs.**

outperforms other robust models by a large margin. This is due to the assumption that pruning links connecting dissimilar ego node features can enhance the adversarial robustness is unsuitable for heterophilic graphs. There already exists a large amount of inter-class links that connect dissimilar ego node features in heterophilic graphs and pruning links according to this strategy may likely delete normal inter-class links. However, **NSPGNN** prunes links based on the aggregated neighbors' feature similarity instead of ego feature similarity and thus can precisely prune the malicious inter-class links, which makes it particularly suitable for enhancing the adversarial robustness of GNNs over heterophilic graphs.

6.2.2 Defense Against Minmax. We also present the adversarial robustness of GNNs against Minmax—another typical graph structural attack method on heterophilic graphs in Tab. 2. Similar to Mettack, it is observed that **NSPGNN** and its ablation consistently outperform other HGNN baselines by a large margin in most cases. For example, the performance gains between **NSPGNN** and the second-best performances for Squirrel with $\delta_{atk} = 1\%$, 5% , 10% , 15% , 20% , 25% are 18.68%, 25.89%, 33.67%, 25.45%, 26.15%, 25.13%. It is demonstrated that preserving the neighbor similarity can also effectively mitigate the malicious effects caused by Minmax. It is worth noting that **NSPGNN** consistently outperforms the HGNN baselines even for the clean graph ($\delta_{atk} = 0\%$). It is probably that

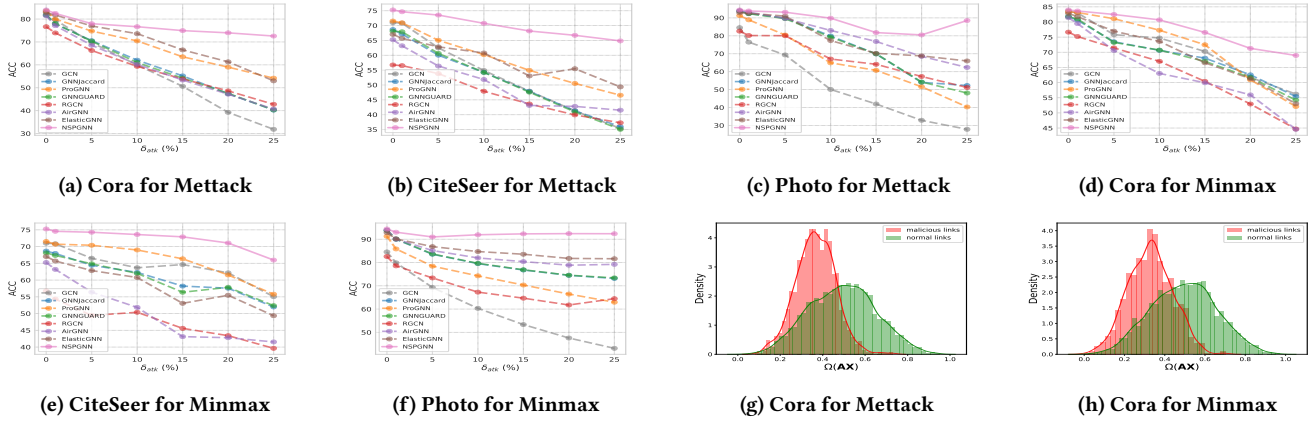


Figure 6: Accuracies under different attacking scenarios on homophilic graphs ((a)-(f)) and density plots for Cora ((g),(h)).

the positive kNN graph construction can serve as a data augmentation technique to refine the clean graph’s structure information and make it particularly suitable for semi-supervised node classification tasks. Overall, the phenomenon that NSPGNN performs the best in most cases both against Mettack and Minmax illustrates that our proposed robust model indeed can effectively provide sufficient valid signals to supervise the propagation, which smooth the distance of intra-class nodes and enlarge the distance of inter-class nodes.

On the other hand, Fig. 5c, 5d, 5e present the robust performances of the proposed method compared with other robust baselines against Minmax. It is observed that NSPGNN significantly outperforms other robust models with different attacking powers. The largest gap between NSPGNN and the second-best performances are 24.24%, 33.41% and 18.86% for Chameleon, Squirrel and Crocodile respectively. In the meanwhile, the performance gaps between the proposed method and other robust models increase as the attacking power increases. This phenomenon demonstrates that preserving neighbor similarity can precisely prune a proportion of malicious effects even when the poisoned graphs are highly contaminated while vanilla robust models fail to effectively mitigate the malicious effects, particularly on highly poisoned graphs.

6.3 Robustness over Homophilic Graphs

In this section, we analyze the adversarial robustness of the proposed model over homophilic graphs and experimentally verify that preserving neighbor similarity can also deal with malicious effects on homophilic graphs. Fig. 6a, 6d, 6b, 6e, 6c, 6f presents the robust performances of the proposed model compared with current robust baselines against graph structural attacks on Cora, CiteSeer and Photo. The observations are two-fold: **1) NSPGNN** consistently achieves the best performances compared to the robust baselines under different attacking scenarios for homophilic graphs. It indicates that preserving neighbor similarity can also mitigate the adversarial effects of graph structural attacks on homophilic graphs and even performs better than preserving ego similarity (GCN-Jaccard, ProGNN, GNNGUARD etc.). This result coincides with the theoretical proof of Theorem. 2 since the theoretical result

is independent of the homophily ratio of the input graph data. 2) Similar to the results in Tab. 2, NSPGNN performs the best among the robust models on homophilic clean graphs, which demonstrates that preserving the neighbor similarity can serve as an effective data augmentation technique to refine the clean graph’s structure for better semi-supervised node classification performances. In contrast, preserving ego similarity such as GCN-Jaccard may sacrifice the clean graph’s accuracy. This phenomenon is supported by Theorem. 2 since the attack loss (negative classification loss) is negatively related to neighbor similarity instead of ego similarity. Thus, preserving ego similarity cannot optimize the classification loss for the clean graph.

6.4 Similarity on Homophilic Graphs

It is previously mentioned in Sec. 4 that the newly defined similarity matrix $\Omega(\mathbf{A}^T\mathbf{X})$ can successfully tell apart the malicious links out of normal links based on the density of the similarity scores for each link. In this section, we additionally explore whether this similarity metric can serve as a malicious effect detector for homophilic graphs. Fig. 6g and 6h provide the density plots of similarity scores for Cora (More results please refer to the appendix). These results indicate that the similarity metric can also distinguish malicious links from normal links on homophilic graphs. Additionally, it can also verify the success of NSPGNN against graph structural attacks on homophilic graphs.

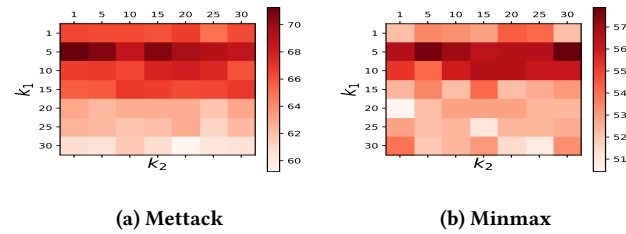


Figure 7: Sensitivity analysis on the number of nearest neighbors for positive kNN graph (k_1) and negative kNN graph (k_2).

6.5 Sensitivity Analysis

In this section, we provide the sensitivity analysis on the number of nearest neighbors of positive kNN graph k_1 and negative kNN graph k_2 . Fig. 7 presents the sensitivity results for Chameleon under attacking power equal to 10% (For more results please refer to the appendix). It is observed that the performance of **NSPGNN** is more sensitive to k_1 than k_2 . This phenomenon indicates that the impact of the positive kNN graph is larger than the negative kNN graph, which coincides with the ablation results.

7 CONCLUSION

In this paper, we investigate the malicious impacts of graph structural attacks and propose a universally robust GNN framework—**NSPGNN** to enhance the adversarial robustness of GNN both on homophilic and heterophilic graphs by preserving the neighbor similarity. To this end, we first provide theoretical and empirical studies on the relationship between neighbor similarity and attack loss and find out that graph structural attacks tend to connect node pairs with dissimilar aggregated neighbors' features. Based on this new insight, we novelly construct a dual-kNN graph pipeline and propagate the node features along the positive kNN graph with the low-pass filter to smooth the features of node pairs with high similarity scores and propagate the nodal features along the negative kNN graph with the high-pass filter to discriminate the node pairs with low similarity scores. As a byproduct, preserving neighbor similarity can also serve as a data augmentation to refine the clean graph's structure for better performances of semi-supervised node classification. Extensive experiments demonstrate the effectiveness of the proposed method against graph structural attacks and improve the clean graph's accuracy both on homophilic and heterophilic graphs.

REFERENCES

- [1] Abien Fred Agarap. 2018. Deep learning using rectified linear units (relu). *arXiv preprint arXiv:1803.08375* (2018).
- [2] Peter W Battaglia, Jessica B Hamrick, Victor Bapst, Alvaro Sanchez-Gonzalez, Vinicius Zambaldi, Mateusz Malinowski, Andrea Tacchetti, David Raposo, Adam Santoro, Ryan Faulkner, et al. 2018. Relational inductive biases, deep learning, and graph networks. *arXiv preprint arXiv:1806.01261* (2018).
- [3] Deyu Bo, Xiao Wang, Chuan Shi, and Huawei Shen. 2021. Beyond low-frequency information in graph convolutional networks. In *Proceedings of the AAAI Conference on Artificial Intelligence*, Vol. 35. 3950–3957.
- [4] Eli Chien, Jianhao Peng, Pan Li, and Olgica Milenkovic. 2021. Adaptive Universal Generalized PageRank Graph Neural Network. In *International Conference on Learning Representations*. <https://openreview.net/forum?id=n6jl7fLxrP>
- [5] Nur Nasuha Daud, Siti Hafizah Ab Hamid, Muntadher Saadon, Firdaus Sahran, and Nor Badrul Anuar. 2020. Applications of link prediction in social networks: A review. *Journal of Network and Computer Applications* 166 (2020), 102716.
- [6] Chenhui Deng, Xiuyu Li, Zhuo Feng, and Zhiru Zhang. 2022. GARNET: Reduced-Rank Topology Learning for Robust and Scalable Graph Neural Networks. In *The First Learning on Graphs Conference*. <https://openreview.net/forum?id=kvwWjYQtmw>
- [7] Lun Du, Xiaozhou Shi, Qiang Fu, Xiaojun Ma, Hengyu Liu, Shi Han, and Dongmei Zhang. 2022. Gbk-gnn: Gated bi-kernel graph neural networks for modeling both homophily and heterophily. In *Proceedings of the ACM Web Conference 2022*. 1550–1558.
- [8] Negin Entezari, Saba A. Al-Sayouri, Amirali Darvishzadeh, and Evangelos E. Papalexakis. 2020. All You Need Is Low (Rank): Defending Against Adversarial Attacks on Graphs. In *Proceedings of the 13th International Conference on Web Search and Data Mining (Houston, TX, USA) (WSDM '20)*. Association for Computing Machinery, New York, NY, USA, 169–177. <https://doi.org/10.1145/3336191.3371789>
- [9] Matthias Fey and Jan E. Lenssen. 2019. Fast Graph Representation Learning with PyTorch Geometric. In *ICLR Workshop on Representation Learning on Graphs and Manifolds*.
- [10] Will Hamilton, Zhitao Ying, and Jure Leskovec. 2017. Inductive representation learning on large graphs. *Advances in neural information processing systems* 30 (2017).
- [11] Simon Haykin. 1994. *Neural networks: a comprehensive foundation*. Prentice Hall PTR.
- [12] Dongxiao He, Chundong Liang, Huixin Liu, Mingxiang Wen, Pengfei Jiao, and Zhiyong Feng. 2022. Block modeling-guided graph convolutional neural networks. In *Proceedings of the AAAI conference on artificial intelligence*, Vol. 36. 4022–4029.
- [13] Wei Jin, Yao Ma, Xiaorui Liu, Xianfeng Tang, Suhang Wang, and Jiliang Tang. 2020. Graph structure learning for robust graph neural networks. In *Proceedings of the 26th ACM SIGKDD international conference on knowledge discovery and data mining*. 66–74.
- [14] Diederik P. Kingma and Jimmy Ba. 2017. Adam: A Method for Stochastic Optimization. *arXiv:1412.6980* [cs.LG]
- [15] Thomas N. Kipf and Max Welling. 2017. Semi-Supervised Classification with Graph Convolutional Networks. In *International Conference on Learning Representations*. <https://openreview.net/forum?id=SJU4ayYgl>
- [16] Jia Li, Yu Rong, Hong Cheng, Helen Meng, Wenbing Huang, and Junzhou Huang. 2019. Semi-supervised graph classification: A hierarchical graph perspective. In *The World Wide Web Conference*. 972–982.
- [17] Jintang Li, Bingzhe Wu, Chengbin Hou, Guoji Fu, Yatao Bian, Liang Chen, Junzhou Huang, and Zibin Zheng. 2023. Recent Advances in Reliable Deep Graph Learning: Inherent Noise, Distribution Shift, and Adversarial Attack. *arXiv:2202.07114* [cs.LG]
- [18] Jia Li, Honglei Zhang, Zhichao Han, Yu Rong, Hong Cheng, and Junzhou Huang. 2020. Adversarial Attack on Community Detection by Hiding Individuals. In *Proceedings of The Web Conference 2020 (Taipei, Taiwan) (WWW '20)*. Association for Computing Machinery, New York, NY, USA, 917–927. <https://doi.org/10.1145/3366423.3380171>
- [19] Qimai Li, Zhichao Han, and Xiao-Ming Wu. 2018. Deeper insights into graph convolutional networks for semi-supervised learning. In *Proceedings of the AAAI conference on artificial intelligence*, Vol. 32.
- [20] Yaxin Li, Wei Jin, Han Xu, and Jiliang Tang. 2020. Deeprobust: A pytorch library for adversarial attacks and defenses. *arXiv preprint arXiv:2005.06149* (2020).
- [21] Xiaorui Liu, Jiayuan Ding, Wei Jin, Han Xu, Yao Ma, Zitao Liu, and Jiliang Tang. 2021. Graph Neural Networks with Adaptive Residual. In *Advances in Neural Information Processing Systems*. A. Beygelzimer, Y. Dauphin, P. Liang, and J. Wortman Vaughan (Eds.). https://openreview.net/forum?id=hfKER_KJiNw
- [22] Xiaorui Liu, Wei Jin, Yao Ma, Yaxin Li, Hua Liu, Yiqi Wang, Ming Yan, and Jiliang Tang. 2021. Elastic graph neural networks. In *International Conference on Machine Learning*. PMLR, 6837–6849.
- [23] Sitao Luan, Chenqing Hua, Qincheng Lu, Jiaqi Zhu, Mingde Zhao, Shuyuan Zhang, Xiao-Wen Chang, and Doina Precup. 2022. Revisiting heterophily for graph neural networks. *Advances in neural information processing systems* 35 (2022), 1362–1375.
- [24] Julian McAuley, Christopher Targett, Qinfeng Shi, and Anton Van Den Hengel. 2015. Image-based recommendations on styles and substitutes. In *Proceedings of the 38th international ACM SIGIR conference on research and development in information retrieval*. 43–52.
- [25] Andrew Kachites McCallum, Kamal Nigam, Jason Rennie, and Kristie Seymore. 2000. Automating the construction of internet portals with machine learning. *Information Retrieval* 3 (2000), 127–163.
- [26] Miller McPherson, Lynn Smith-Lovin, and James M Cook. 2001. Birds of a feather: Homophily in social networks. *Annual review of sociology* 27, 1 (2001), 415–444.
- [27] Gary L. Miller, Shang-Hua Teng, William Thurston, and Stephen A. Vavasis. 1997. Separators for Sphere-Packings and Nearest Neighbor Graphs. *J. ACM* 44, 1 (jan 1997), 1–29. <https://doi.org/10.1145/256292.256294>
- [28] Ryan A. Rossi and Nesreen K. Ahmed. 2015. The Network Data Repository with Interactive Graph Analytics and Visualization. In *AAAI*. <https://networkrepository.com>
- [29] Nino Shervashidze, Pascal Schweitzer, Erik Jan Van Leeuwen, Kurt Mehlhorn, and Karsten M Borgwardt. 2011. Weisfeiler-lehman graph kernels. *Journal of Machine Learning Research* 12, 9 (2011).
- [30] Naoki Shibata, Yuya Kajikawa, and Ichiro Sakata. 2012. Link prediction in citation networks. *Journal of the American society for information science and technology* 63, 1 (2012), 78–85.
- [31] Amit Singhal et al. 2001. Modern information retrieval: A brief overview. *IEEE Data Eng. Bull.* 24, 4 (2001), 35–43.
- [32] Laurens Van der Maaten and Geoffrey Hinton. 2008. Visualizing data using t-SNE. *Journal of machine learning research* 9, 11 (2008).
- [33] Mark Weber, Giacomo Domeniconi, Jie Chen, Daniel Karl I Weidele, Claudio Bellei, Tom Robinson, and Charles E Leiserson. 2019. Anti-money laundering in bitcoin: Experimenting with graph convolutional networks for financial forensics. *arXiv preprint arXiv:1908.02591* (2019).
- [34] Felix Wu, Amauri Souza, Tianyi Zhang, Christopher Fifty, Tao Yu, and Kilian Weinberger. 2019. Simplifying Graph Convolutional Networks. In *Proceedings of the 36th International Conference on Machine Learning (Proceedings of Machine Learning Research, Vol. 97)*, Kamalika Chaudhuri and Ruslan Salakhutdinov (Eds.). PMLR, 6861–6871. <https://proceedings.mlr.press/v97/wu19e.html>
- [35] Huijun Wu, Chen Wang, Yuriy Tyshetskiy, Andrew Docherty, Kai Lu, and Liming Zhu. 2019. Adversarial Examples for Graph Data: Deep Insights into Attack and Defense. In *Proceedings of the Twenty-Eighth International Joint Conference on Artificial Intelligence, IJCAI-19*. International Joint Conferences on Artificial Intelligence Organization, 4816–4823. <https://doi.org/10.24963/ijcai.2019/669>
- [36] Zonghan Wu, Shirui Pan, Fengwen Chen, Guodong Long, Chengqi Zhang, and S Yu Philip. 2020. A comprehensive survey on graph neural networks. *IEEE transactions on neural networks and learning systems* 32, 1 (2020), 4–24.
- [37] Kaidi Xu, Hongge Chen, Sijia Liu, Pin-Yu Chen, Tsui-Wei Weng, Mingyi Hong, and Xue Lin. 2019. Topology Attack and Defense for Graph Neural Networks: An Optimization Perspective. In *Proceedings of the Twenty-Eighth International Joint Conference on Artificial Intelligence, IJCAI-19*. International Joint Conferences on Artificial Intelligence Organization, 3961–3967. <https://doi.org/10.24963/ijcai.2019/550>
- [38] Xiang Zhang and Marinka Zitnik. 2020. GNNGUARD: Defending Graph Neural Networks against Adversarial Attacks. In *Proceedings of the 34th International Conference on Neural Information Processing Systems (Vancouver, BC, Canada) (NIPS'20)*. Curran Associates Inc., Red Hook, NY, USA, Article 777, 13 pages.
- [39] Ziwei Zhang, Peng Cui, and Wenwu Zhu. 2020. Deep learning on graphs: A survey. *IEEE Transactions on Knowledge and Data Engineering* 34, 1 (2020), 249–270.
- [40] Jie Zhou, Ganqu Cui, Shengding Hu, Zhengyan Zhang, Cheng Yang, Zhiyuan Liu, Lifeng Wang, Changcheng Li, and Maosong Sun. 2020. Graph neural networks: A review of methods and applications. *AI open* 1 (2020), 57–81.
- [41] Dingyuan Zhu, Ziwei Zhang, Peng Cui, and Wenwu Zhu. 2019. Robust Graph Convolutional Networks Against Adversarial Attacks. In *Proceedings of the 25th ACM SIGKDD International Conference on Knowledge Discovery & Data Mining (Anchorage, AK, USA) (KDD '19)*. Association for Computing Machinery, New York, NY, USA, 1399–1407. <https://doi.org/10.1145/3292500.3330851>
- [42] Jiong Zhu, Yujun Yan, Lingxiao Zhao, Mark Heimann, Leman Akoglu, and Danai Koutra. 2020. Beyond homophily in graph neural networks: Current limitations and effective designs. *Advances in neural information processing systems* 33 (2020), 7793–7804.
- [43] Yulin Zhu, Yuni Lai, Kaifa Zhao, Xiapu Luo, Mingquan Yuan, Jian Ren, and Kai Zhou. 2022. BinarizedAttack: Structural Poisoning Attacks to Graph-based Anomaly Detection. In *2022 IEEE 38th International Conference on Data Engineering (ICDE)*. 14–26. <https://doi.org/10.1109/ICDE53745.2022.00006>
- [44] Daniel Zügner, Amir Akbarnejad, and Stephan Günnemann. 2018. Adversarial Attacks on Neural Networks for Graph Data. In *SIGKDD*. 2847–2856.
- [45] Daniel Zügner and Stephan Günnemann. 2019. Adversarial Attacks on Graph Neural Networks via Meta Learning. In *International Conference on Learning Representations*. <https://openreview.net/forum?id=Bylnx209YX>

A DATASET DESCRIPTION

More descriptions on three heterophilic graphs—Chameleon, Squirrel and Crocodile and three homophilic graphs—Cora, CiteSeer and Photo are presented in Tab. 3.

Table 3: Dataset statistics.

Datasets	N	$ \mathcal{E} $	Classes	Features	$\mathcal{H}(G)$
Chameleon	2277	31371	5	2325	0.23
Squirrel	5201	198353	5	2089	0.22
Crocodile	11631	170773	5	128	0.23
Cora	2485	5069	7	1433	0.74
Citeseer	2110	3668	6	3703	0.81
Photo	7650	119081	8	745	0.60

B BASELINES

The baselines include the state-of-the-art GNN variants for heterophilic graphs and robust GNN models.

- **GCN** [15] is the most representative GNN model which utilizes the graph convolutional layer to propagate node features with a low-pass filter.

The following are GNNs under heterophily:

- **GPRGNN** [4] adaptively learns the generalized PageRank weights to optimize nodal feature and topological information extraction jointly.
- **FAGNN** [3] adaptively integrates low-pass and high-pass signals in the message-passing mechanism to learn graph representations for homophilic and heterophilic graphs.
- **H2GCN** [42] identifies ego- and neighbor-embedding separation, higher-order neighborhoods, and a combination of intermediate representations to boost learning from the graph structure under heterophily.
- **GBKGNN** [7] proposes a bi-kernel feature transformation and a selection gate to capture homophily and heterophily information respectively.
- **BMGNN** [12] introduces block modeling into the framework of GNN to automatically learn the corresponding aggregation rules for neighbors of different classes.
- **ACMGNN** [23] proposes the adaptive channel mixing framework to adaptively exploit aggregation, diversification and identity channels node-wisely to extract richer localized information for diverse node heterophily situations.
- **GARNET** [6] is a scalable spectral method to leverages weighted spectral embedding to construct a base graph, and then refines the base graph by pruning additional uncritical edges based on a probabilistic graphical model.

The following are robust GNN models:

- **GCN-Jaccard** [35] preprocesses the graph data by pruning links that connect nodes with low values of Jaccard similarity of node attributes.
- **ProGNN** [13] jointly learns a structural graph and a robust GNN model from the poisoned graph guided by the three properties: low-rank, sparsity and feature smoothness.
- **GNGUARD** [38] detects and quantifies the relationship between the graph structure and node features to assign higher

weights to edges connecting similar nodes while pruning edges between unrelated nodes during training.

- **RGCN** [41] learns Gaussian distributions for each node feature and employs an attention mechanism to penalize nodes with high variance.
- **AirGNN** [21] proposes an adaptive message passing scheme to learn a GNN framework with adaptive residual to tackle the trade-off between abnormal and normal features during GNN training.
- **ElasticGNN** [22] to enhance the smoothness of the graph data locally and globally by L_1 and L_2 penalties to enhance the adversarial robustness of the GNN framework.

C ALGORITHMS

Alg. 1 presents the algorithm details of NSPGNN.

Algorithm 1 NSPGNN.

Require: Input graph adjacency matrix \mathbf{A} and its attributes \mathbf{X} , hyperparameters k_1 and k_2 , training labels \mathbf{Y}_{tr} , node-set \mathcal{V} , learning rate η , training epoch T , number of hidden layers L , parameters set Θ .

- 1: **Bi-kNN graph pipeline:**
 - 2: Compute similarity matrix:

$$\Omega(\mathbf{A}^\tau \mathbf{X})[u, v] = \frac{\mathbf{A}^\tau \mathbf{X}[u]^\top \cdot \mathbf{A}^\tau \mathbf{X}[v]}{\|\mathbf{A}^\tau \mathbf{X}[u]\| \cdot \|\mathbf{A}^\tau \mathbf{X}[v]\|},$$
 - 3: Obtain positive kNN graphs:

$$\mathbf{A}^{kNN_\tau}[u] \in \text{Argsort_Desc}_{v \in \mathcal{V} \setminus u} \Omega(\mathbf{A}^\tau \mathbf{X})[u, v],$$
 - 4: Obtain negative kNN graphs:

$$\mathbf{A}^{kNN_r}[u] \in \text{Argsort_Asc}_{v \in \mathcal{V} \setminus u} \Omega(\mathbf{A}^\tau \mathbf{X})[u, v].$$
 - 5: **Neighbor-Similarity-Guided Propagation:**
 - 6: **for** $t \leq T$ **do**
 - 7: Initialize $\mathbf{H}^{(0)} = \mathbf{X}$,
 - 8: **for** $l = 1, 2, \dots, L$ **do**
 - 9: Obtain learnable weights:

$$[\alpha_1^{(l)}, \alpha_2^{(l)}] = \sigma(\mathbf{H}^{(l-1)} \mathbf{W}_m^{(l)} + \mathbf{b}_m^{(l)}),$$

$$[\beta_1^{(l)}, \beta_2^{(l)}] = \sigma(\mathbf{H}^{(l-1)} \mathbf{W}_n^{(l)} + \mathbf{b}_n^{(l)});$$
 - 10: Obtain positive and negative propagation matrix:

$$\hat{\mathbf{A}}^{p(l)} = \alpha_1^{(l)} \odot \hat{\mathbf{A}}^{kNN_1} + \alpha_2^{(l)} \odot \hat{\mathbf{A}}^{kNN_2},$$

$$\hat{\mathbf{A}}^{n(l)} = \beta_1^{(l)} \odot \hat{\mathbf{A}}^{nkNN_1} + \beta_2^{(l)} \odot \hat{\mathbf{A}}^{nkNN_2},$$
 - 11: Obtain node embeddings via guided propagation: $\mathbf{H}^{(l)} = \sigma(\mathbf{H}^{(l-1)} \mathbf{W}_s^{(l)} + \hat{\mathbf{A}}^{p(l)} \mathbf{H}^{(l-1)} \mathbf{W}_o^{(l)} + (\mathbf{I} \hat{\mathbf{A}}^{n(l)}) \mathbf{H}^{(l-1)} \mathbf{W}_d^{(l)}).$
 - 12: Gradient descent: $\Theta^t \leftarrow \Theta^{t-1} - \eta \frac{\partial \mathcal{L}_{nll}(\mathbf{H}^{(L)}, \mathbf{Y}_{tr})}{\partial \Theta}$.
 - 13: **end for**
 - 14: **end for**
 - 15: **return** NSPGNN node embeddings $\mathbf{H}^{(L)}$.
-

D ADDITIONAL DENSITY PLOTS

Fig. 8 presents the density plots of the defined similarity scores with $\tau = 1$ (Eqn. 10) for malicious links and normal links of homophilic graphs—CiteSeer and Photo. It indicates that the similarity score can also tell apart malicious links from normal links for CiteSeer and Photo.

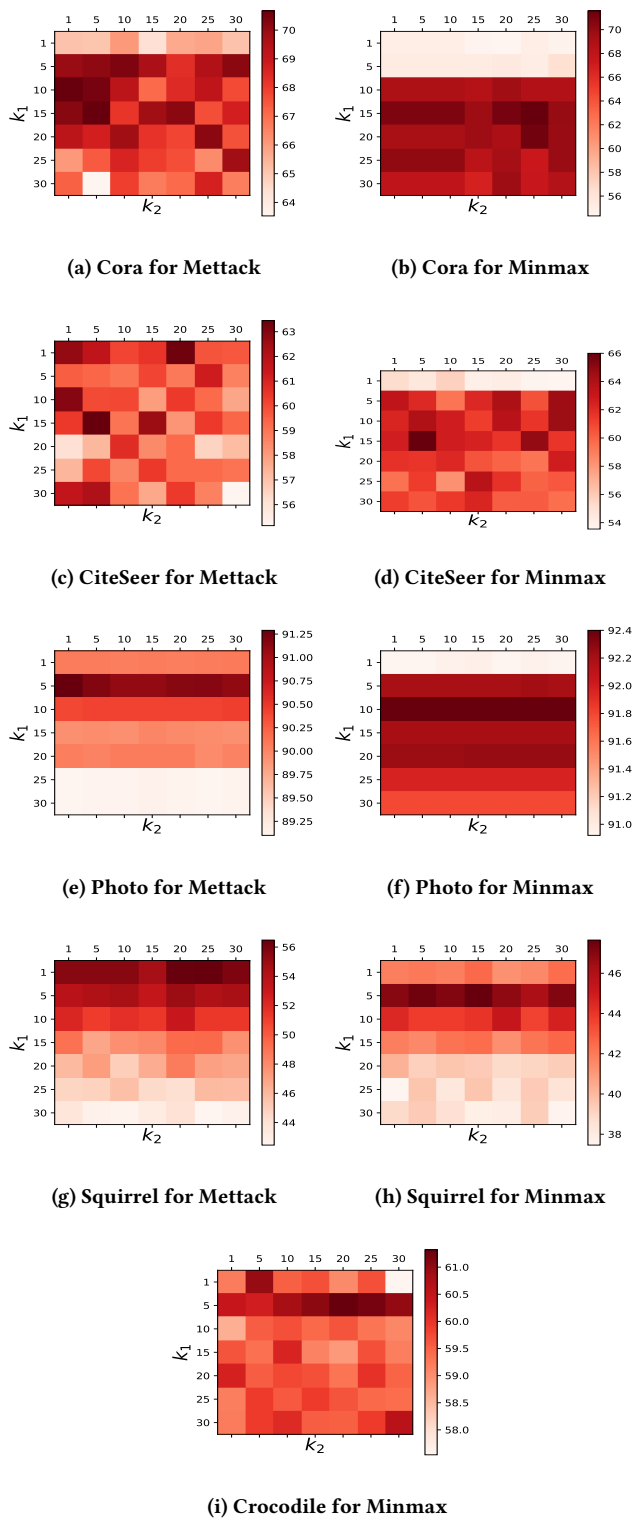


Figure 9: Sensitivity.

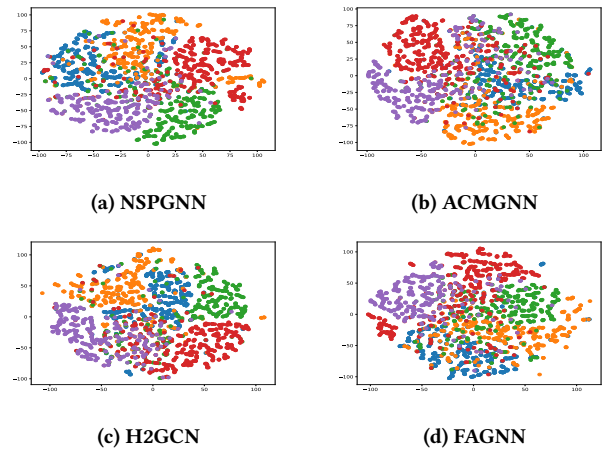


Figure 10: Embed.

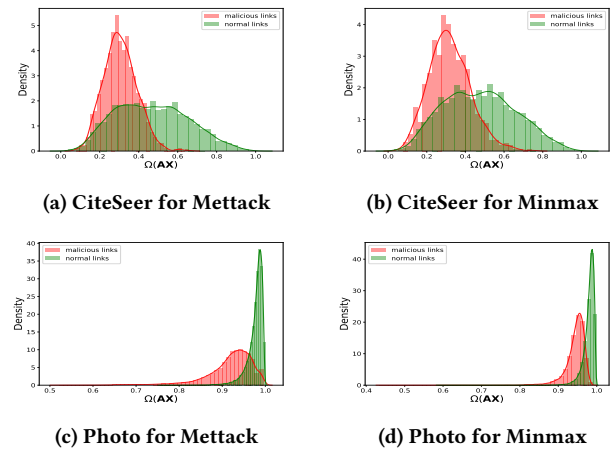


Figure 8: Density plots of similarity scores for malicious links and normal links of poisoned CiteSeer and Photo.

D.1 Additional Sensitivity Analysis

Fig. 9 provides the sensitivity analysis on the hyperparameters k_1 and k_2 for Cora, CiteSeer, Photo, Squirrel and Crocodile. It is observed that the proposed model is more sensitive to k_1 than k_2 in most cases both for homophilic and heterophilic graphs. On the other hand, the significant row-wise performance gap for different k_1 implies that choosing an appropriate k_1 is important for better robust performance.

E NODE EMBEDDINGS VISUALIZATION

Fig. 10 presents the scatterplot of the node embeddings of NSPGNN and other baselines under 25% Mettack. The node embeddings are pre-processed by t-SNE [32]—a typical dimension reduction technique for easy data visualization. It is observed that the distribution of the representations of the proposed method forms more separable decision boundaries than baselines, which demonstrates the effectiveness of preserving the neighbor similarity.